Journal of Alloys and Compounds, 182 (1992) 35–42
JALCOM 110

A15 structure formation in Ti–Pd

A. F. Jankowski
Lawrence Livermore National Laboratory, Chemistry and Materials Science, PO Box 808, Livermore, CA 94550 (USA)

(Received May 22, 1991)

Abstract

Vapor phase formation of thin films in the Ti–Pd alloy system is investigated using magnetron sputter deposition. Crystalline as-deposited structures are produced with nominal compositions of 20, 25 and 30 at.%Pd. The high temperature b.c.c. phase is produced on room temperature substrates via quenching from the vapor phase. An A15 structure of Ti_3Pd is rigorously identified for the first time, in agreement with predictions from electronic structure calculations.

1. Introduction

The existence of low temperature metastable phases and accompanying transformations are approachable using thin films. Vapor deposition is useful for preparing alloys with specific composition and crystallographic structure. Thin films are especially convenient for direct examination using *in situ* hot stage electron microscopy and X-ray diffraction. Thin film preparation techniques can provide unusual metastable starting materials which are typically unattainable using conventional bulk processing.

The Ti–Pd system is chosen to study the short-range order which develops in the b.c.c. solid solution above or near the possible domain existence of the long-range order of an A15 structure. Previous study of the Ti–Pd system for palladium concentrations greater than 33 at.% produced the formation of an amorphous phase with subsequent crystallization and ordering upon *in situ* heating [1, 2]. Current examination of alloys with concentrations less than 33 at.% Pd will allow for the experimental feasibility of studying ordering near the proposed A15 phase. Electronic structure calculations [3, 4] do suggest the existence of an A_3B-type phase. In comparison, the reported A15 structure at 20 at.% Pd (*i.e.* Ti_4Pd) in current phase diagrams [5] is apparently speculative, since no conclusive experimental evidence exists in reports [2, 6] of this off-stoichiometric phase.

2. Synthesis

Planar magnetron sputtering in the d.c. mode is used as the vapor deposition method. A compositionally homogeneous solid is attainable using

0925-8388/92/$5.00

TABLE 1

Palladium composition (atomic per cent) of Ti–Pd films

Nominal composition	Analysis method		
	Crystal monitor	AES	STEM
30	29.5	28.8	32.8
25	23.5	25.2	28.2
20	20.8	20.3	23.5

a "multilayer" approach. A sequential deposition of titanium and palladium is monitored and controlled to produce the desired film stoichiometry. By alternating the source materials to produce near-submonolayer thick layers, an atomic-scaled intermixing is formed in the deposited film.

A three-source multilayer deposition system is used to fabricate films 0.23–0.26 μm thick. Substrates of Si(111) and cleaved mica, mounted on a copper platen of diameter 30 cm, are sequentially passed (at 0.012 rev s^{-1}) 20 cm over each of three planar magnetrons. Of the three sources used, two are for titanium, the major constituent, and the third is for palladium. Operating target voltages of 195–200 and 260 V are used for the titanium and palladium magnetrons respectively. The contribution in thickness from each source is constant and ranged from 0.1 to 0.3 nm rev^{-1}. The base pressure of the deposition chamber is 7×10^{-8} Torr. A 5 mTorr working pressure of argon is maintained with a 25.5 cm^3 min^{-1} flow of gas from a liquid argon Dewar. The appearance and color of the as-deposited foils are specular and silver metallic. The compositions of the foils (listed in Table 1) are determined from profilometer-calibrated quartz crystal monitors. The substrate temperature did not exceed 71 °C for any deposition run.

3. Characterization and analysis

3.1. X-ray diffraction (XRD)

The Ti–Pd films are removed from the mica substrates by immersion in an 80 °C distilled water bath. The foils are placed on a glass slide and allowed to dry. The foils are initially examined using a powder diffractometer with a graphite monochromator and Cu Kα X-rays. Low angle (grazing incidence) θ–2θ scans did not reveal reflections characteristic of an artificial composition modulation. This result is expected for these samples since submonolayer contributions from each deposition source are intended to produce a homogeneous foil composition. High angle θ–2θ scans indicate textured, crystalline Ti–Pd deposits. The single high intensity Bragg reflection (as for the nominal 25 at.%Pd foil of Fig. 1) does not readily permit crystal structure identification.

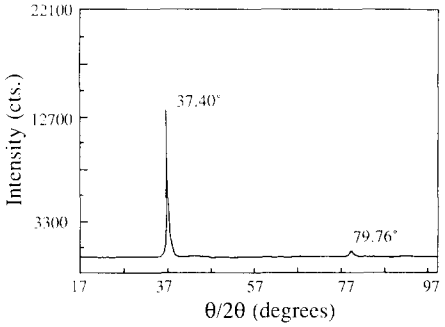

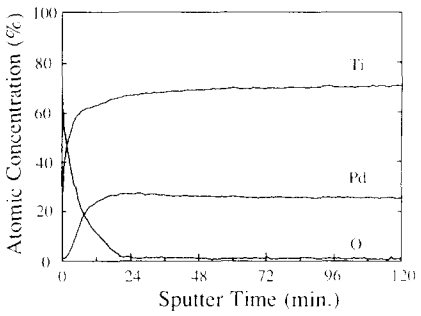

Fig. 1. Cu Kα X-ray diffraction θ–2θ scan indicating that the as-deposited Ti–Pd film with nominal 25 at.%Pd is crystalline and highly textured.

Fig. 2. AES composition profile of as-deposited Ti–Pd film with nominal 25 at.%Pd indicating a uniform concentration of titanium and palladium. Surface contamination of oxygen is completely removed 20 min into the profile.

3.2. Auger electron spectroscopy (AES)

The uniformity of composition through the as-deposited coating is measured over a 25 mm^2 area using Auger depth profiling. The surface is bombarded with a 3 keV, 10 μA electron beam, resulting in the ejection of Auger electrons with energies characteristic of each element (*i.e.* 330 eV for palladium and 418 eV for titanium). A 5 keV, 1.16 μA argon ion beam is used to sputter etch through the sample. The pressure for sputter etching is 2×10^{-5} Torr, whereas the system base pressure is 5×10^{-10} Torr. Calculation of the concentration is based on the energy peak heights (within a 10–20 eV window of the characteristic peak) of data acquired in the derivative mode. The Auger composition profiles (as for the nominal 25 at.% Pd foil of Fig. 2) produce atomic per cent palladium concentrations (listed in Table 1) consistent with values obtained from the calibrated quartz crystal monitors. Apparent near-surface contamination from oxygen is completely removed shortly into the depth profile.

3.3. Transmission electron microscopy (TEM)

The Ti–Pd films floated off the mica substrates are examined in plan view using bright field (BF) imaging and selected area diffraction (SAD). The crystal structure of the deposits will be analyzed using the SAD patterns. The planar spacing corresponding to the principal reflection in each SAD pattern is equated with the accurate planar spacing measured for that reflection in the XRD θ–2θ scans. Samples from each nominal composition are examined in the as-deposited state then annealed *in situ*. A single tilt temperature stage in a JEOL-200CX side-entry transmission electron microscope is used to study any ordering which occurs from the as-deposited crystalline state. Heating rates of 2–10 °C min^{-1} are used to increase the sample temperature from 25 °C to a maximum of 725 °C in these experiments. An energy-dispersive spectrometer (EDS) is used in the scanning transmission electron microscopy (STEM) imaging mode for composition analysis of the as-deposited

films (listed in Table 1). The 4.51 keV Ti K and 2.82 keV Pd L lines are used (as shown in Fig. 3) in the semiquantitative analysis. The STEM composition data obtained are affected by less than 1 at.% for an absorption correction.

The BF image of the as-deposited Ti–Pd film with a nominal 30 at.% Pd composition reveals a nanocrystalline structure (Fig. 4a) with a grain size less than 10 nm. The SAD pattern (Fig. 4b) can be indexed, using the most basic interpretation, as a b.c.c. structure with a lattice parameter of 0.345 nm. The (110) reflection (of 100% intensity) is accompanied by the (211) and (220) reflections (of weak intensity). The sample is then heated *in situ* to 550 °C for 10 min and allowed to cool to 250 °C for imaging. The annealing temperature of 550 °C is chosen to induce any phase transformation which may occur, such as that originally postulated for the observance of short-range order prior to transformation to an A15 structure. In addition, the 550 °C annealing temperature remains below the temperature of 595 °C which induces phase separation to Ti_2Pd and α-Ti. The BF image (Fig. 4c) of the heated sample shows the formation of a second phase which is identified in the [−1 3 3] pole projection of the SAD pattern (Fig. 4d) as Ti_2Pd. The Ti_2Pd identification is confirmed by successively orienting the sample to the [−1 1 3] and [0 −1 0] pole projections. No intermediate phase (*i.e.* A15) is observed during this annealing treatment. After an additional anneal for 10 min at 550 °C, diffuse rings from the (101) and (211) reflections of α-TiPd become evident.

The BF image of the as-deposited Ti–Pd film with a nominal 25 at.% Pd composition reveals a nanocrystalline structure (Fig. 5a) with a grain size less than 10 nm. The SAD pattern (Fig. 5b) can only be completely indexed to an A15 structure with a lattice parameter of 0.482 nm. A possible fit to the α-TiPd phase [7] is not likely owing to discrepancies in the planar spacings for (101) and (311) as shown in Table 2. The sample is then annealed *in situ* at 550 °C for 5 min, at which point ordering to Ti_2Pd was observed in the SAD pattern.

The BF image of the as-deposited Ti–Pd film with a nominal 20 at.% Pd composition reveals a nanocrystalline structure (Fig. 6a) with a grain

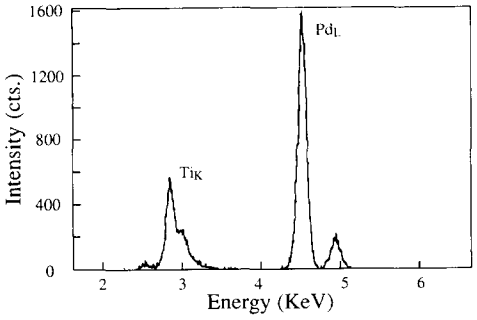

Fig. 3. STEM-mode-generated EDS data accumulated during a scan duration of 646 s from as-deposited Ti–Pd film with nominal 25 at.%Pd.

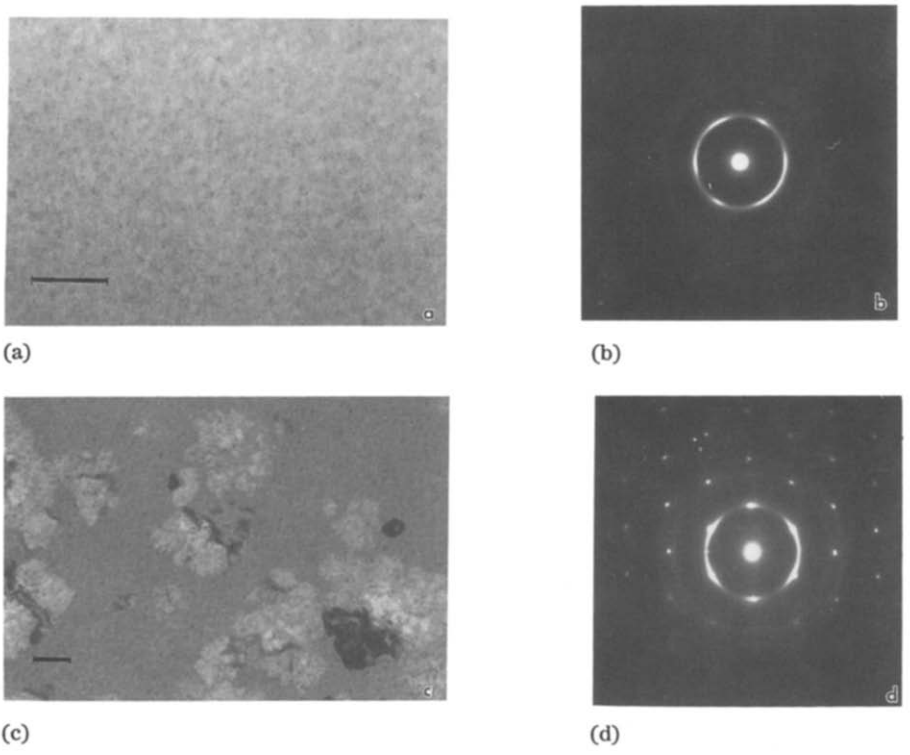

(a) (b)

(c) (d)

Fig. 4. TEM imaging of nominal 30 at.%Pd film (a) as deposited in BF, (b) as deposited in SAD, (c) after 550 °C anneal in BF and (d) after 550 °C anneal in SAD. The bar represents 0.1 μm.

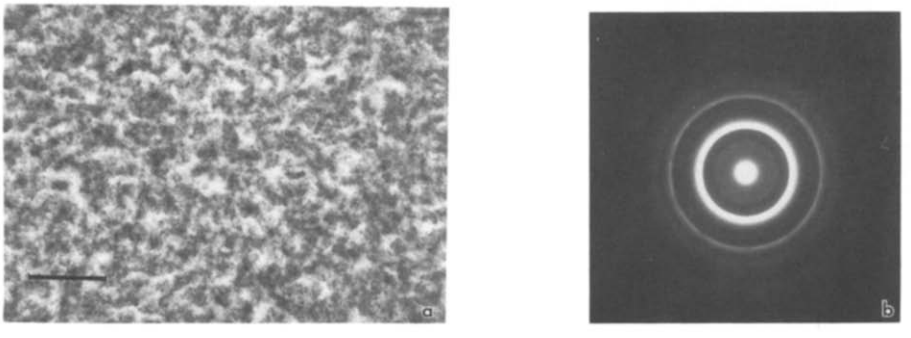

(a) (b)

Fig. 5. TEM imaging of nominal 25 at.%Pd film as deposited in (a) BF and (b) SAD. The bar represents 0.1 μm.

size of 20 nm. The SAD pattern (Fig. 6b) can be indexed as a b.c.c. structure with a lattice parameter of 0.322 nm. The (110) reflection (of 100% intensity) is accompanied by the (200), (211), (220), (310), (222) and (321) reflections. The sample is then heated *in situ* to 450 °C for 15 min and allowed to cool

TABLE 2

Planar spacings (nanometres) and (*hkl*) of the 25 at.% Pd film with possible identification as A15 or α-TiPd

A15 ($\alpha = 0.482$)	As deposited	α-TiPd
0.341 (110)	0.3399	0.332 (101)
0.241 (200)	0.2403	0.243 (011)
0.2155 (210)	0.2155	0.215 (111)
0.170 (220)	0.1640	0.1665 (211)
0.139 (222)	0.1394	0.141 (020)
0.134 (320)	0.1336	0.129 (311)
0.1205 (400)	0.1212	0.1195 (220)
0.114 (330)	0.1152	0.1175 (?)
0.108 (420)	0.1064	

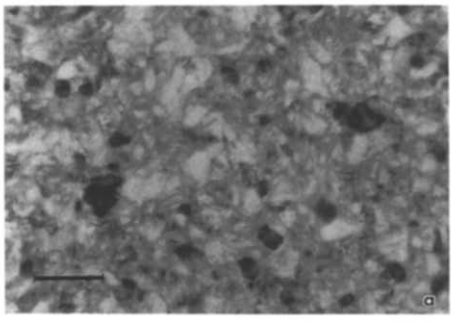

(a)

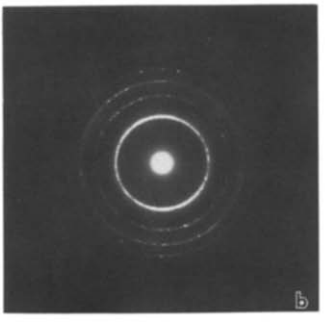

(b)

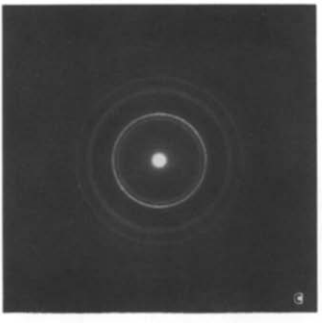

(c)

Fig. 6. TEM imaging of nominal 20 at.%Pd film (a) as deposited in BF, (b) as deposited in SAD and (c) after 725 °C anneal in SAD. The bar represents 50 nm.

to 250 °C for imaging. The grain size increases, intensifying the b.c.c. reflections. Additional annealing for 5 min at 670 °C and for 5 min at 725 °C induces the transformation to Ti_2Pd as seen in the SAD pattern (Fig. 6c). No intermediate phase (*i.e.* A15) is observed during this annealing treatment.

4. Discussion

The formation of the b.c.c. structures in the Ti–Pd films with nominal 20 and 30 at.%Pd compositions occurs as a result of direct quenching from the vapor, *i.e.* the solid solution equivalent of the high temperature β-Ti phase. The nanocrystalline structure is a direct result of such a quenching process. The lattice parameter for the 20 at.%Pd film follows a Vegard's rule-of-mixtures value, whereas the 30 at.%Pd sample shows a positive deviation. The formation of the A15 structure is found at 25 at.%Pd on a room temperature substrate. The lack of any observation of the b.c.c. structure transforming to an A15 structure before forming the Ti_2Pd structure indicates that the A15 phase field is confined between approximately 23 and 28 at.% Pd. The observation of ordering to the Ti_2Pd structure at temperatures above 550 °C but not below 450 °C indicates that a tie-line to the Ti_2Pd phase occurs between 450 and 550 °C and not at 595 °C as indicated in the established phase diagram [5]. These new results are incorporated into the phase diagram for Ti–Pd (Fig. 7).

To substantiate the present equilibrium revisions to the Ti–Pd phase diagram (in Fig. 7), an additional thermal aging treatment is conducted using the Ti–Pd foils. A 450 °C vacuum anneal (at 1.8×10^{-7} Torr) for 70 h is used, to accommodate kinetic considerations, in the stabilization of the phases present at the tie-line above the A15 phase. Characterization of the samples is again accomplished using selected area electron diffraction. In brief, for each Ti–Pd foil the α-TiPd and Ti_2Pd phases are found in addition to the b.c.c. (for the 23 and 28 at.%Pd samples) or A15 (for the 25 at.%Pd sample) parent phase.

In summary, an A15 structure of Ti_3Pd is rigorously identified for the first time. The observed A15 structure of Ti_3Pd is in agreement with predictions from electronic structure calculations [3, 4]. Observations of ordering from the b.c.c. structure to an A15 phase may be possible by vapor depositing films on cryogenically cooled substrates. In this way a b.c.c. parent phase

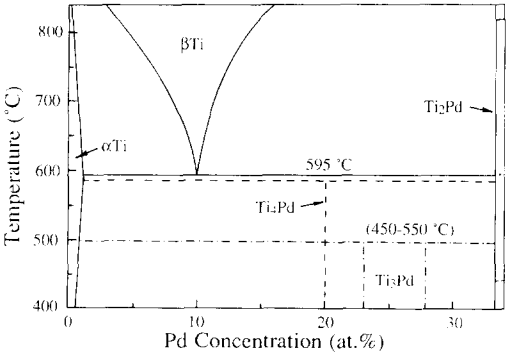

Fig. 7. Phase diagram for Ti–Pd with palladium concentrations less than 34 at.%, modified to include the A15 phase as found in this report (– · –) and as previously [5] represented (– – –).

may form for Ti–Pd films with compositions between 23 and 28 at.%Pd, *i.e.* 25 at.%Pd.

Acknowledgments

The following individuals are thanked for their contribution to this effort: L. Schrawyer (AES) and M. Wall (TEM). This work was performed under the auspices of the United States Department of Energy by Lawrence Livermore National Laboratory under contract W-7405-Eng-48.

References

1 A. F. Jankowski, M. A. Wall and P. E. A. Turchi, *J. Less-Common Met., 161* (1990) 115.
2 S. Zhang, K. Sumpiyama and Y. Nakamura, *Mater. Trans. JIM, 30* (1989) 733.
3 P. E. A. Turchi, G. Treglia and F. Ducastelle, *J. Phys. F: Met. Phys., 13* (1983) 2543.
4 A. Finel and F. Ducastelle, *M. R. S. Symp. Proc., 21* (1984) 293.
5 T. B. Massalski (ed.), *Binary Alloy Phase Diagrams*, American Society for Metals, Metals Park, OH, 1986, p. 1878.
6 E. Raub and E. Roschel, *Z. Metal., 59* (1968) 112.
7 *JCPDS-ICDD File No. 19-895*, 1988.